Newtonian and non-Newtonian CFD Models of Intracranial Aneurysm: A Review

Samar A. Mahrous[1,2,*], Nor Azwadi Che Sidik[1,3], Khalid M. Saqr[2,4]

1   Department of Thermo-fluid Universiti Teknologi Malaysia, 81310 UTM Skudai, Malaysia
2   College of Engineering and Technology, Arab Academy for Science, Technology and Maritime Transport, P.O.BOX 1029 Alexandria, Egypt
3   Malaysia – Japan International Institute of Technology (MJIIT), University Teknologi Malaysia Kuala Lumpur, 54100 Kuala Lumpur, Malaysia
4   Research Center for Computational Neurovascular Biomechanics (RCCNB), Alexandria University Hospital in Smouha, 21554 Alexandria, Egypt

ARTICLE INFO	ABSTRACT
	Computational Fluid Dynamics (CFD) has become an essential research tool to investigate the physical, biophysical and pathophysiological processes leading to the formation, growth and rupture of intracranial aneurysms (IAs). The diverse anatomical complexities of IAs dictate a staggering level of sophistication inherited in the CFD modeling process. From medical imaging to wall shear stress mapping on the aneurysm walls, there are numerous physical assumptions related to blood flow and wall dynamics. The majority of such assumptions remain controversial until today. This review is an endeavor to summarize, in a critical and comprehensive manner, the different assumptions used to calculate blood viscosity in CFD models of IA hemodynamics. The tabulated summaries of literature presented herein also highlight the inconsistency of location choice and imaging techniques used to select IA models for CFD studies. This review presents a roadmap for the state-of-the art knowledge about blood viscosity models used with IA CFD models, and suggests future research directions to further characterize the nature of blood flow which contributes to the improvement of diagnosis and management of IAs.

1. Introduction

In order to establish the importance of viscosity models in CFD simulations of IAs, the flow physics, mechanobiology and pathophysiology of IAs must be comprehended. Blood is multiharmonic pulsatile flow that exhibits a multitude of complex phenomena which flowing in complex arterial geometries. Endothelial cells (ECs) respond to different regimes of blood flow in numerous mechanisms that are being investigated until the present moment.

IA is a complex vascular disorder that involves blood flow dynamics, ECs mechanotransduction as well as vascular pathology. Any CFD simulation is a simplification of this multilayered complexity. The use of viscosity model, nevertheless, controls the outcome of such simulation in quantitative manner

---

* *Corresponding author.*
E-mail address: samar.mahrous@aast.edu (Samar A. Mahrous)

and in some qualitative aspects as well. This introduction serves as a brief instructive summary of such topics in order to show the importance of viscosity models in IAs CFD simulations.

Studies revealed that subarachnoid hemorrhage (SAH) occurred in 6 to 20 cases out of 100,000 individuals all over the world [1]. It is found that 30,000 people in the United States suffer from a brain aneurysm rupture, while, in Egypt according to the Official national statistics people suffer from cerebral aneurysm rupture may be around 150 000 to 210 000. In addition, Studies revealed that the cerebral aneurysm ruptures every 18 minutes in the US [2]. Serious disability or sudden death may result, depending on the severity of the hemorrhage. SAH has an overall mortality of approximately 40% to 50% [1] and case-fatality rates varied between 32% and 67% [3]. There are two main types of intracranial aneurysms: saccular and fusiform. The former type represents more than 90% of intracranial aneurysms [4], having berry-like, spherical, sharply circumscribed sacs connected to the vessel by a neck. The most common location of saccular aneurysms arise from the arteries in the subarachnoid space at the base of the brain called the "circle of Willis" [5, 6].

An aneurysm is a weak area in a blood vessel that usually enlarges [7]. It is often developed when the arterial wall becomes too weak to resist hemodynamic forces [8, 9]. The genesis, growth and rupture risk of intracranial aneurysms (IAs) are affected by blood flow in arteries, which exhibits complex physical phenomena [10, 11]. Flow conditions in the IA are among the main reasons of the lumen's endothelium dysfunction. IAs are normally found at the apex of bifurcations of the main arteries, at the origin of small arteries branching from large ones. Moreover, it can be found on the sidewall of arteries with sharp bends [12-14]. It is defined by the deterioration of the cerebrovascular wall that shows loss of the internal elastic lumina, disruption of the tunica media, and the death of mural cells [15-18]. These are often followed by remodeling and degradation of extracellular matrix (ECM) proteins throughout the arterial wall which renders them strongly susceptible to further proinflammatory responses which are thought to be driven by wall shear stress (WSS) [19, 20]. There are two parameters that have been correlated to the evolution of the aneurysm, which are: high WSS and low WSS. Both have been linked with endothelial dysfunction [21, 22] while the former was linked to arterial wall remodeling. The latter is related to the blood flow recession area in the dome as a result of the stagnated flow inside the aneurysm which could contribute to the thinning, damage and subsequent rupture of the aneurysmal wall [8, 9, 23-25]. The flow dynamics' changes during the development of the aneurysm have been evaluated and results showed that there is a considerably low WSS at the evolution area [26-28]. Figure 1 shows a mechanistic chart of IA pathobiology presenting in parallel the stress factors and wall alterations, that gradually cause changes in the IA morphology. The repetitive pressure and the disturbed WSS cause a gradual enlargement on the vessel wall. This can lead to loss and degeneration of the internal elastic lamina IEL as a result of hypertension, atherosclerosis and turbulent flow, followed by the disruption of the tunica media thus promote mural cell death in the IA [15-18]. These have been followed by remodeling and degradation of extracellular matrix (ECM) proteins throughout the arterial wall [19]. Therefore, the death of mural cell is the main event that renders the wall strongly susceptible to rupture risk [29].

The objective of the present work is to review the investigations of computational flow dynamics by focusing on CFD studies in intracranial aneurysms and comparing the different viscosity models used to simulate the blood flow. The structure of this article is as follows: Section 2 reviews CFD role in investigating cerebral aneurysms, Section 3 presents hemodynamic approaches, including the Newtonian and non-Newtonian models, and finally, Section 4 summarizes the main remarks.
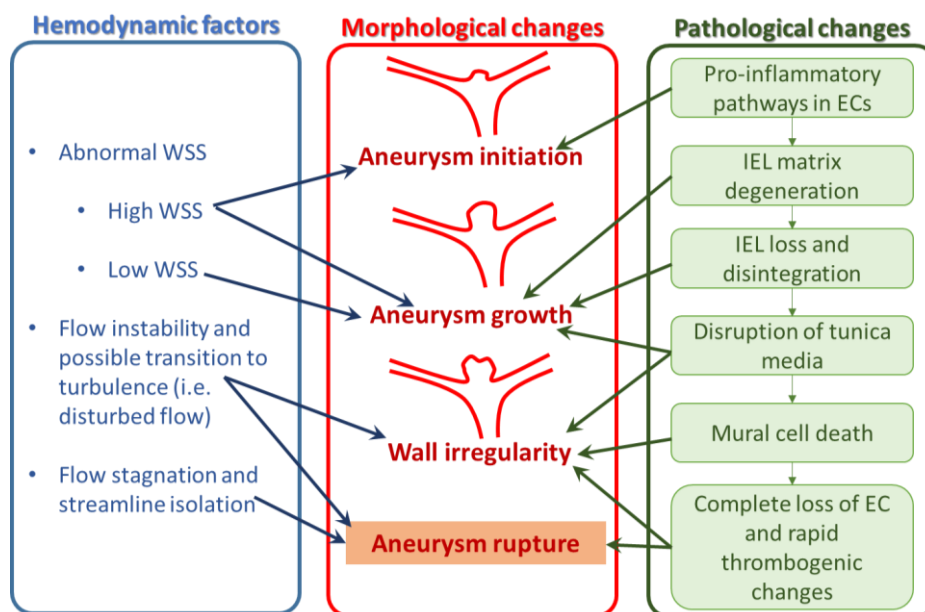
Fig. 1. Mechanisms of IA initiation, growth and rupture. Many factors and correlations in such mechanisms are still under investigation

2. CFD as A Research Tool in IA Hemodynamics

For the past two decades, Computational Fluid Dynamics (CFD) has been the most prominent research tool for investigating the effect of fluid dynamics in intracranial aneurysms and any possible geometry [30, 31]. CFD is increasingly relied upon for elucidating blood flow dynamics in cerebral aneurysms [18, 32], such as the WSS, the mean wall shear stress (MWSS), the time average wall shear stress (TAWSS) and the oscillatory shear index (OSI) [33] and their possible role in determining rupture risk. Most studies assumed that the fluid flow in human body is laminar [34]. The Reynolds number in cerebral vessels is in the order of 100, which marks laminar pulsatile flow according to the classical theory of hydrodynamics. However, recent high-resolution CFD studies have shown the existence of unstable flow and possible transitional or turbulent flow in some cerebral aneurysms at such low Reynolds number [35, 36], which is unjustifiable by the hydrodynamic stability theory. This observation suggests that a much more emphasis on transition in the computational simulation community might be necessary. The possible consequences of the presence of transitional or turbulent flow on such pathologies is that, it leads to a deleterious mechanotransduction resulting in remodeling and degeneration of the arterial wall. In addition, the unpredictability of transitional flow may even be a feature that aggravate the state.

Most of CFD studies of cerebral aneurysm hemodynamics focus on analyzing the blood flow characteristics and their effect on the aneurysm wall dynamics. The majority of numerical simulations of intracranial aneurysm, have assumed the blood as Newtonian fluid when solving the Navier-Stokes equation for both the steady and pulsatile flows [8, 37-40]. It is nearly a consensus that the alterations of blood viscosity are inconsiderable. However, some groups reported the significance of non-Newtonian effects in intracranial blood flow [41-47].
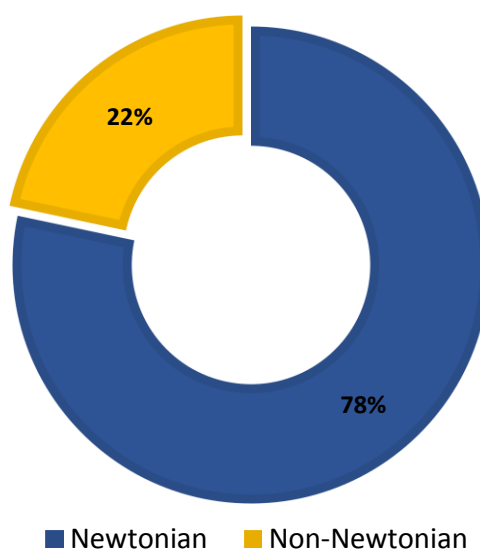
Currently, there is no complete theory which can predict the impacts of the blood rheology on the hemodynamics in cerebral aneurysms. To that end, it is clear that in order to understand the initiation and progression of intracranial aneurysm, it is crucial to investigate the effects of different blood viscosity models on the intra-aneurysmal hemodynamics.

Understanding the physics of this lesion formation can lead to the right prognosis of the disease which resulted in more frequent detection of cerebral aneurysm before rupture that assist in limiting the devastating effects of this disorder and guide to possible therapies.

In addition, another factor affecting the intra-aneurysmal flow is the selection of the image acquisition datasets and post-processing, because it may yield sources of errors as inaccurate numerical simulations results. Berg *et al.,* [48] reported that the choice of the data acquisition impact the hemodynamic simulation mostly in the small blood vessels. Moreover, Geers *et al.,* [49] examined four patient specific MCA aneurysms by comparing the effect of two image modalities (CTA and 3DRA). They demonstrated agreement of the qualitative flow characteristics. However, they found considerable conflicts quantitatively in the measurements. Furthermore, there was an overestimation of the aneurysm neck size illustrated by Schneiders *et al.*, [50] based on 2D-DSA and 3DRA comparisons in 20 patients. They found that this neck size overestimation can have non-trivial consequences on hemodynamics simulations such as different flow structure characteristics and significant differences regarding the WSS results.

2.1 BLOOD Rheology Constitutive Equations

There has been a number of controversies concerning the fundamental physical assumptions underlying aneurysm hemodynamics simulations. A comprehensive meta-analysis survey is conducted to summarize these controversies. Figure 2 shows a classification of the literature surveyed on Scopus© bibliographic database according to (a) the method of investigation and (b) the blood viscosity assumption used in the CFD models of intracranial aneurysms. Syntactic searches used to classify literature based on TITLE-ABS-KEY fields as following: (1) (TITLE-ABS-KEY ("cerebral aneurysm" OR "intracranial aneurysm") AND TITLE-ABS-KEY ("computational fluid dynamics" OR "CFD" OR "numerical simulation")) (2) ((TITLE-ABS-KEY ("cerebral aneurysm" OR "intracranial aneurysm") AND TITLE-ABS-KEY ("computational fluid dynamics" OR "CFD" OR "numerical simulation"))) AND ("non-Newtonian"). It can be seen that non-Newtonian models constitute 23% of the CFD studies. Later in the present review, the differences between such models and Newtonian assumptions will be highlighted.

Fig. 2. Qualitative statistics on literature of the blood viscosity models adopted in CFD simulations of IA

3. Hemodynamics Approaches

Blood is responsible for transporting nutrients via a complex mixture of cells, proteins, lipoproteins, and ions and removing wastes [51]. The blood in the heart and large arteries is usually modeled as Newtonian and this hypothesis may be acceptable in a lot of cases. However, in other cases, this assumption is not precise, especially when examining the flow in small arteries [40, 52, 53].

3.1 Newtonian Approach

Most studies of intracranial hemodynamics depended on assuming blood as Newtonian fluid and that the variations of blood viscosity are unimportant. Some of these studies have not discussed the fact of this assumption at all [54-56]. While other studies mentioned that the vessel diameter is large enough to disregard the non-Newtonian behavior of blood [28, 57]. The value of shear rate in which the blood was assumed to be Newtonian changes according to different studies, for example: in Ref. [52] the value was 45 s^{-1}, in Ref. [58] the value was 50 s^{-1} ,while another studies set the shear rate greater than 100 s^{-1} [53]. The Newtonian viscosity assumption of blood is only valid in large arteries (>10 mm diameter) (e.g. aorta), because in large arteries the rheological properties of blood become linear [59]. In some studies blood was simulated as Newtonian fluid with constant viscosity ranging from 3.5 mPa to 5 mPa as stated by several authors [60-67] and some other studies simulate blood with another values of viscosity as in Refs. [68, 69]. Saqr *et al.,* [70] showed, using in-vivo Transcranial Doppler ultrasound measurements that the use of Newtonian model to calculate WSS results in significant differences with commonly used non-Newtonian models in CFD.

Several researches performed to study the intracranial aneurysm rupture risk. Some of these studies based on the morphological changes, for example, the impact of change of the size or the geometry of the intracranial aneurysm on the flow pattern [25, 71-77]. In addition, other studies focused more on the effect of hemodynamics factors such as, wall shear stress (WSS), oscillatory shear index (OSI), inflow jet sizes and impingement regions on the behavior of the flow [28, 37, 54, 78-86].

3.1.1 Morphological studies using newtonian viscosity model

It is important to mention that intra-aneurysmal hemodynamics are substantially dependent on the morphology of intracranial aneurysm and its parent artery [38, 87, 88].

Stojanović *et al.,* [71] analyzed 114 patients suffered from ruptured IA. The study examined the association between the rupture risk and the existence of aneurysmal changes on the cerebral vessels. Then concluded that high incidence of asymmetrical configuration in the circle of Willis among patients with ruptured aneurysms suggest the possible relation between asymmetrical configuration and disturbance in hemodynamic with genesis and rupture of IA. Kayembe *et al.,* [72] demonstrated that any change from the optimal geometry would contribute to increment in WSS levels which prone to aneurysm initiation and growth. Cebral *et al.,* [89] investigated the hemodynamics of four cerebral aneurysms models with respect to the flow division, the mesh size the viscosity model and the effect of geometry. It was found that the intra-aneurysmal characteristics do not considerably differ when changing the mean flow rate. For the mesh resolution, three grids were used. A coarse grid with 0.5 million elements, a medium grid with 1.25 million elements and a fine grid with 4.61 million elements, and it was found that the important characteristics of the flow can be captured regardless the mesh size. Regarding the viscosity model, it was observed that the

main flow features of the basilar artery aneurysm was the most affected case by the use of Casson viscosity model, because the flow rate is relatively small. However, the rest of the cases were not affected by using the non-Newtonian viscosity model. Finally, the most effective parameter that was found to alter the actual intra-aneurysmal hemodynamics and expect the eventual rupture was the geometry. Chien *et al.,* [80] analyzed 24 patient specific models using 3DRA. These selected cases were collected from November 2007 to June 2008. They used the 6-region method to study the hemodynamics properties at the peak systole of the second cardiac cycle of two cardiac cycles computed. It was observed quantitative alterations in WSS and flow rate which is relative to aneurysm location. However, no considerable relation was found between the intra-aneurysmal hemodynamic and the parent artery size. In addition, results revealed that WSS was high in the arteries compared with the aneurysm. The average WSS obtained was 10.3 ± 5.2 Pa. High WSS and flow rate were recorded in the MCA aneurysms. While, the lowest values of WSS and flow rate were recorded at the basilar artery, followed by the AcomA and ICA aneurysms. In addition, it was found that the flow in the MCA aneurysms was faster than that of the AcomA aneurysms. A computational analysis of a developing cerebral aneurysm is presented. The blood flow pattern, WSS distribution and the geometric progression have been investigated using the 3D computed tomographic angiography 3DCTA [25]. It was observed that the aneurysm was developed and exposed to a relatively high WSS, resulting in a geometric change of the proximal parent artery, which caused significant alterations in the aneurysm hemodynamic.

Parent artery has a major effect on the intra-aneurysmal fluid dynamics. Castro *et al.,* [74] have proved that the torsion of the upstream artery can crucially affect the IA hemodynamics. The Womersley profile has been used to study the effect of the geometry of the upstream parent artery on the intra-aneurysmal flow dynamics in 4 patient-specific cerebral aneurysms under pulsatile flow [74]. It was observed that the variations found in the intra-aneurysmal fluid dynamics essentially were due to the geometry of the main vessel. Following that, the hemodynamic patterns exhibited areas of high WSS in the aneurysm dome and complex flow. Whereas, Wang, *et al.,* [75] studied the influence of aneurysm geometry on the hemodynamics by altering the aneurysm diameter and the aspect ratio (AR), where the aspect ratio (AR), defined as IA maximum height divided by the average neck diameter as shown in figure 3. This study showed that the WSS is globally reduced and the wall pressure on the aneurysm is increased with increasing AR. However, no such alteration is found when increasing the sac diameter for constant AR.

Moreover, the influence of changing the radius and the bifurcation angle of the artery in the circle of Willis on the WSS and the pressure has been estimated, based on patient-specific data [76]. This study showed that deviations from normal anatomy lead to redistribution of wall pressures and increased WSS with larger branching angle. The estimated peak values for WSS were greater than 30 Pa, which is counted sufficient to cause the degeneration of the endothelial cell, weakness of the arterial wall and consequently aneurysmal growth. Additionally, the wall tension and the wall displacement in intracranial aneurysms have been determined based on patient-specific geometry with flexible walls [77]. The analysis showed that the WSS and the shape of the aneurysm most probably are very significant factors that lead to aneurysm evolution and rupture.

The most studied parameter of the IA morphology is the IA size. Even though large aneurysms in diameter more than 10 mm are found to be dangerous. In fact, numerous studies have revealed that a great percentage of ruptured intracranial aneurysms are less than 10 mm in size [88, 90-95]. Moreover, several studies noted that there is a relation between the position of the vessel and the IA rupture [74, 80, 94, 96]. These findings emphasize the significance of the vessel morphology and location on the IA hemodynamics and rupture risk.
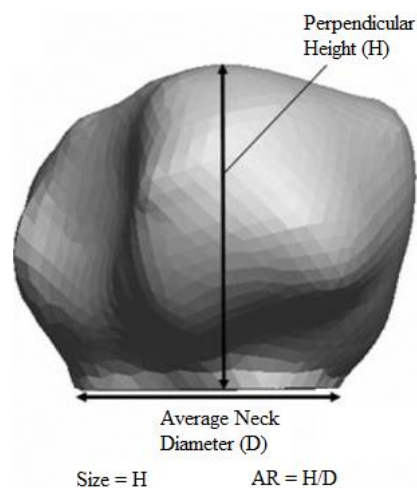
Fig. 3. Definition of the aneurysm geometric aspect ratio on a DSA image

3.1.2 Hemodynamic studies using newtonian model

Blood hemodynamics have been demonstrated to play a significant role in IA pathophysiology and eventual rupture. Several studies focused on the influence of hemodynamics factors on the flow pattern of IA by assuming blood as Newtonian fluid.

Intracranial aneurysms were studied using the 3D rotational angiography 3DRA in 62 patient-specific models to investigate the relation between the flow dynamic inside the aneurysm and the risk of its rupture assuming blood as Newtonian [37]. This study revealed that 72% of ruptured aneurysms had complex or disturbed flow patterns, 80% had small impaction zones, and 76% had narrow inflows. While, the unruptured aneurysms had 73% simple stable flow patterns, 82% had high impaction zones and 75% had large inflows. In addition, they found that aneurysms with small impaction regions were 6.3 times more likely to be ruptured than those with large impingement sizes. The hemodynamics in 3 saccular cerebral aneurysms with a terminal morphology imaged just prior its rupture has been examined taking into account the Newtonian properties of blood and the pulsatile flow condition [79]. It was observed that the following hemodynamics were correlated with the high risk of rupture which are concentrated inflow jet that affects a relatively small area of the aneurysmal wall, complex flow structure, elevated levels of WSS in proximity of the impingement region and low WSS in the most of the aneurysm sac. The flow dynamics of 26 anterior communicating artery AcomA aneurysms has been examined. Many of these aneurysms correlated with previous history of rupture [97]. The findings of this study are aneurysms with small impingement regions, large jet size and consequently higher MWSS were more probable to be burst. In addition, MWSS can be used as a sign responsible of aneurysmal future rupture.

Although a high WSS plays a main role in the genesis of CA, a low WSS might be a major factor for its growth. The magnitude and direction of the WSS in and around saccular cerebral aneurysms in 20 middle cerebral aneurysms have been analyzed, using the 3D computed tomographic angiography 3DCT [81]. This study found that the magnitude of the WSS of the aneurysm zone is significantly lower than that of the vessel area. The low WSS may be one of the essential factors underlying the degeneration of the aneurysmal wall. The influence of hypertension and smoking on WSS at the site of cerebral aneurysm has been investigated [83]. They found that long-term vulnerability to elevated WSS as a result of smoking and hypertension can be a possible culprit in the evolution of intracranial aneurysm. Furthermore, the greatest values of WSS at aneurysm formation

area were about 5 times greater than the average values in the parent arteries. The association between low WSS and aneurysm development in seven patient-specific models of cerebral aneurysms has been determined [28]. Results revealed that the magnitude of WSS inside the aneurysm is significantly low and this low WSS leading to endothelial dysfunction and may be an important contributor to the remodeling of the arterial vessel wall and to aneurysm development and rupture. The relationship between the local hemodynamics and the initiation of blebs in 20 cerebral aneurysms has been investigated [98]. It is found that blisters created at or close to zones of high WSS in most cases. In addition, this study revealed that locally increased WSS could lead to arterial wall deterioration which created these blebs. The hemodynamic conditions of 3 saccular aneurysms have been examined. The change in dynamic pressure and WSS that take place due to alterations in pulsatile blood flow has been studied when a patient exercise [84]. It was shown that the overall flow was not substantially changed during moderate aerobic exercise. Furthermore, the WSS and the pressure on the aneurysmal wall did not significantly differ between rest and exercise.

Seven cases of aneurysms treated with flow diversion have been studied to investigate the possible rupture mechanisms by comparing 3 ruptured aneurysms with 4 aneurysms with successful treatment using 3DRA [56]. The hemodynamics including pressure and WSS were analyzed. Blood flow was modeled as unsteady, Newtonian fluid. From this study, the intra-aneurysmal pressure is increased which may be the cause of subsequent aneurysmal bleeding, especially in giant aneurysms. In addition, significant decrease in the overall WSS and a slow intra-aneurysmal circulation were observed in the cases of post-treated rupture. The influence of the surgical treatment on the flow pattern in an enormous fusiform cerebral aneurysm has been studied by using ideal geometry [86]. The finding revealed that the hemodynamic forces that exist through the aneurysmal region are substantially different when the flow in the feeding vessels changes. Moreover, the simulations demonstrated that there would have been a pronounced large jet size, high WSS and associated high-pressure zone on the aneurysmal wall. In that case, blockage of the stenotic artery would greatly lessen the flow influence on the aneurysm wall.

Flow instabilities have been shown to occur in intracranial aneurysms in vitro and in vivo. Valen-Sendstad *et al.,* [78] analyzed whether turbulence can occur in a patient-specific middle cerebral artery (MCA) aneurysm using a pulsatile inflow velocity. The study demonstrated that blood flow exhibited a non-laminar behavior and tends to be turbulent just after peak systole, before relaminarization. Furthermore, it was observed that the WSS showed complex and chaotic behavior at the aneurysm dome. Baek *et al.,* [85] investigated the flow instabilities and pulsatile behavior of WSS on three patient-specific saccular aneurysms at the internal carotid artery. They proposed that the oscillatory behavior of WSS vectors might play a key role in the initiation of a cerebral aneurysm.

All mentioned studies using Newtonian model for simulating blood to study difference cases of aneurysm with patient specific (as shown in Table 1 and Table 2). In addition, in most literature, the blood was modeled as Newtonian which is not entirely correct as the blood viscosity changes in non-linear way with the shear rate. Figure 4 presents the relation between the different blood viscosity models and the shear rate [99]. It can be seen that, the viscosity of the Newtonian model is constant, while, for the different non-Newtonian shear thinning models, the viscosity increases as shear rate decreases especially at low shear rate below 100 s^{-1}.

Table 1

Summary of steady CFD studies utilizing Newtonian models for intracranial aneurysm

Ref	Model and geometry	Aneurysm location	Study objective	Imaging technique used for model extraction	Summary of findings
[71]	114 patient-specific	45 AcomA 30 MCA 16 ICA 17 PcomA 4 PerA 2 VB	Examine the relationship between burst aneurysms and the morphological changes in intracranial arteries	Preoperative cerebral angiography	Morphological changes might, partially, generate alterations in hemodynamic, which responsible for the aneurysm initiation
[75]	Ideal	1 ICA	Study the effect of aneurysm geometry on the hemodynamics by changing the Aspect Ratio (AR) of the aneurysm	The pressure-velocity coupling was decoupled by using the SIMPLEC	The WSS is globally reduced and the wall pressure on the aneurysm is intensified with increasing AR
[86]	1 Patient-specific	1 BA	Model the possible alterations of the flow field that would result from surgical intervention	Using contrast-enhanced 3D MR angiography	A pronounced high velocity jet, increased WSS and associated high-pressure zone on the contralateral aneurysm wall

Table 2

Summary of unsteady CFD studies utilizing Newtonian models for intracranial aneurysm

Ref	Model and Geometry	Aneurysm location	Study objective	Imaging technique used for model extraction	Summary of findings
[25]	1 Patient-specific	1 BA	Investigate the blood flow pattern, the WSS distribution and the geometric progression of a growing aneurysm	using the 3D computed tomographic angiography (3D-CTA)	Significant alterations in the aneurysm hemodynamics, as a result of the geometric change of the proximal parent artery
[28]	7 Patient-specific	3 BA 3 ICA 1 MCA	Determine the association between low WSS and intracranial aneurysms development	Using contrast-enhanced 3D MR angiography	The low WSS has been reported to have a negative effect on endothelial cells which may be an important contributor to aneurysm growth and rupture
[37]	62 Patient-specific	22 ICA 1 AcomA 9 PA 13 PcomA 14 MCA	Study the relation between intra-aneurysmal hemodynamic characteristics and the rupture of cerebral aneurysms	using the 3D rotational angiography (3D-RA)	Aneurysms with small impingement sizes were 6.3 times more likely to rupture than those with large impingement sizes
[76]	10 Patient-specific	BA PA PcomA PCA	Estimate the effect of variations in vessel radii and bifurcation angles on WSS and pressure in the circle of Willis	Using CTA, MRA, and DSA	Deviations from normal anatomy lead to redistribution of wall pressures and increased

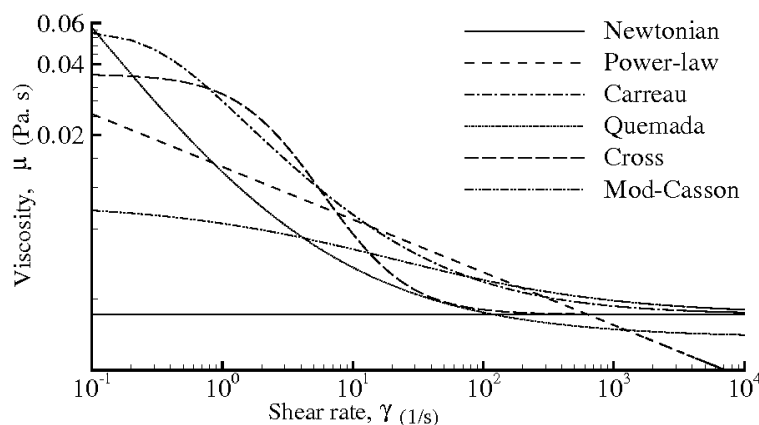|					
					WSS with the larger branching angle. Thus, cause eventual aneurysmal growth
[77]	1 Patient-specific	1 MCA	Determine wall tension in cerebral aneurysms based on patient specific geometry	Using computed tomography angiogram images	WSS is highest near the neck of the aneurysm, and that WSS probably lead to the growth of the aneurysm
[78]	1 Patient-specific	1 MCA	Determine whether turbulence can occur in a middle cerebral artery (MCA) aneurysm	using the 3D computed tomographic angiography (3D-CTA)	The blood flow exhibited a non-laminar behavior and tends to be turbulent
[79]	3 Patient-specific	2 MCA 1 BA	Analyze the hemodynamics in a saccular intracranial aneurysm with a terminal morphology	using the 3D rotational angiography (3D-RA)	The aneurysm had a concentrated inflow jet, complex intra-aneurysmal flow pattern and elevated levels of WSS near the impaction region
[81]	20 Patient-specific	20 MCA	Analyze the magnitude of the WSS in and around saccular cerebral aneurysms	using the 3D computed tomographic angiography (3D-CTA)	The excessively low WSS may be one of the essential factors underlying the aneurysmal growth. Although a high WSS plays a main role in the genesis of CA
[83]	2 Patient-specific	2 ICA	Investigate the influence of smoking and hypertension on WSS at the site of cerebral aneurysm formation	using the 3D rotational angiography (3D-RA)	Long-term vulnerability to elevated WSS as a result of smoking and hypertension can be the main cause in CA evolution
[84]	3 Patient-specific	3 MCA	Investigate intra-aneurysmal alterations in dynamic pressure and WSS that occur when a patient exercises	Using Rotational 3D digital subtraction angiograms	WSS and pressure did not significantly differ between rest and moderate exercise. Time-averaged WSS increased by a mean of 20%
[85]	3 Patient-specific	3 ICA	Investigate the hemodynamics and pulsatile behavior of WSS in intracranial aneurysms	NA	The aneurysmal flow becomes unstable during the decelerating systolic phase. Therefore, both the magnitude and the directions of WSS vectors oscillate at the range of 20–50 Hz
[97]	26 Patient-specific	26 AcomA	Examine the flow dynamics of anterior communicating artery (AcomA) aneurysms	using the 3D rotational angiography (3D-RA)	Aneurysms with small impaction zones, higher inflows, and, consequently, higher MWSS were more likely to be ruptured. Moreover, MWSS potentially could be used as a predictor of aneurysm rupture

Fig. 4. Shear-rate dependent viscosity as described by different non-Newtonian models [99]

The viscosity of the power law model increases, at low shear rate. However, at high shear rate it reduces linearly. In the power law model, it is feasible to get many analytical solutions to the governing equations. Nevertheless, it is failed to characterize the blood at quite high or low shear rates. In addition, the Walburn and Schneck model considered as the extension of the power law model, which depends on the haematocrit of the blood. Moreover, it is found that the blood viscosity in the Casson and Carreau models has a tendency to the asymptotic viscosity at shear rate greater than 10^4 s^{-1}. On the other hand, the Cross and Quemada models show the shear-thinning characteristics at shear rate less than 10^2 s^{-1}. It is noted that the range of non-Newtonian shear rate lies between 0.1 s^{-1} and 10^2 s^{-1} according to Johnston *et al.,* [60].

3.2 Non-Newtonian Approach

Blood flow is a multiphase non-Newtonian pulsatile flow. Blood is composed of red blood cells (RBCs) and white blood cells such that they are elastic cells suspended in a Newtonian liquid known as plasma (continuous phase). Due to the multiphase nature of blood, it is clearly obvious that the blood viscosity will be controlled by the behavior of its microstructural components which are the suspended cells (RBCs). It is found that at low shear rates the RBCs exhibits a behavior known as aggregation, such that the red blood cells start to act like a solid and this will lead to an increase in the blood viscosity. Conversely, as the shear rate increases the RBCs aggregation will be broken and the blood viscosity will decrease. Essentially, blood viscosity is not only affected by the cell aggregation, but it depends on other parameters such as the physiological flow conditions, shear rate, cell shape, plasma viscosity, flow geometry, hematocrit, temperature, cell deformation and orientation. In addition, blood viscosity models can be divided into two main categories which are the Newtonian and the non-Newtonian viscosity models [100]. Blood flow in small arteries often exhibits non-Newtonian characteristics [101-104]. The shear-thinning viscosity models might be rational for flow pattern that have persistent recirculation zones such as aneurysms [105]. In addition, Robertson *et al.,* [23] and Rayz *et al.,* [106] have shown that the use of non-Newtonian viscosity models is merely significant on blood hemodynamics when elevated stagnant zones are found [51]. Furthermore, Arzani [107] concluded that the non-Newtonian models are only suitable for simulating blood flow in aneurysms when high residence-time is found at areas of low shear rates so the RBCs have much time to form rouleaux. In order to determine the most suitable model for simulating the changes of viscosity in blood stream, several non-Newtonian models have been investigated [108-110] (as seen in Table 3). Various models to study blood as non-Newtonian model

used in previous studies and there will be a comparison (as shown in table 4) between different models of non-Newtonian used in simulation of intracranial aneurysm [111, 112].

Table 3
Summary of CFD studies utilizing non-Newtonian models for intracranial aneurysm

Ref	Model and Geometry	Aneurysm location	Study objective	Imaging technique used	Limitations	Summary of findings
[32]	2 patient-specific	1 MCA 1 AcomA	The study aimed to find a relation between the genesis and evolution of the daughter saccules and the hemodynamics	3D-RA	• Non-Newtonian fluid using Carreau-Yasuda model • Pulsatile inlet flow	The high OSI is responsible for the development of the daughter saccule, and the flow inside the aneurysm was more complex and chaotic which lead to aneurysm rupture
[44]	Patient-specific	NA	Investigate the influence of blood viscosity on intra-aneurysmal flow dynamics in coiled aneurysms	3D- RA	• A Newtonian and a non-Newtonian fluid using Casson model	The assumption of a Newtonian fluid can be used in the high-viscous regions
[47]	3 Patient-specific	3 ICA	Analyze the sensitivity of blood flow pattern, shear rate and WSS distributions using different blood viscosity models in realistic intracranial aneurysm geometries	Using Three-dimensional angiography images	• Three rheology models: • Newtonian viscosity model and two non-Newtonian models (Casson and Herschel-Bulkley) • Unsteady flow	Newtonian fluid assumption is satisfactory in CFD simulation of healthy vessels. Although, the non-Newtonian properties of blood should be taken into account in low shear flow (<100/s)
[89]	4 Patient-specific	3 ICA 1 SCA	A study of the sensitivity of the hemodynamic change was carried out in the aneurysm	3D-RA	• A Newtonian and a Non-Newtonian fluid using Casson model • Unsteady model	The most important factor that has the highest effect on the intra-aneurysmal flow patterns is the geometry of the aneurysm and the connected vessels
[102]	Ideal	NA	Examine the effect of non-Newtonian behavior on hemodynamics of intracranial aneurysms of varying morphology	NA	• Four models are investigated: the casson, the generalized power law, and the two forms of the carreau models. • Pulsatile inlet flow	All the non-Newtonian models report a lower WSS than that obtained with a Newtonian model in the same geometry
[124]	Ideal	NA	Examine the influences of non-	CFD	• Non-Newtonian fluid using	Non-Newtonian and pulsatile effects are

			Newtonian viscosity and flow pulsatility to discriminate the stent designs		power law model • Unsteady flow • Rigid walls • Uniform inlet velocity	important to include in order to avoid underestimating of WSS and to discriminate more effectively between stent designs
[126]	1 patient-specific	1MCA	The effect of the blood rheology on the WSS has been evaluated	3D-RA	• A Newtonian and a Non-Newtonian fluid using Carreau-Yasuda fluid model • Unsteady flow	The oscillatory WSS that indicate the damage of the aneurysm is 0.94 Pa in the Carreau-Yasuda case and 1.56 Pa in the Newtonian case
[128]	Patient-specific	NA	A Carreau–Yasuda model was applied to capture the non-Newtonian rheology of blood, and the WSS was compared for both Newtonian and non-Newtonian flows at different Reynolds numbers	3D-MRA	• Non-Newtonian fluid using carreau-Yasuda model. • Constant inlet velocity	The Carreau-Yasuda model leads to a lower viscosity near the walls and a lower WSS comparing with Newtonian flow
[129]	Patient-specific	NA	Study the wall shear stress distribution in a cerebral aneurysm using the lattice Boltzmann method	3D-MRA	• Non-Newtonian fluid using carreau-Yasuda model • Constant inlet velocity	It can be observed that the maximum value of the WSS is overestimated by approximately 30%, if non-Newtonian effects are not taken into consideration
[130]	1 Patient-specific	1 ICA	Study the influences of non-Newtonian blood properties on flow patterns and wall shear stress	3D-RA	• A Newtonian and a Non-Newtonian fluid using Herschel–Bulkley fluid model • Unsteady flow	The impact of shear-thinning behavior on WSS showed significant alterations only in regions with high velocity gradients than Newtonian model
[131]	3 patient-specific	3 ICA	Examine the effects of WSS that may contribute to aneurysm formation	3D-DSA	• Non-Newtonian fluid using Carreau model • unsteady flow	WSS oscillated between a maximum and minimum value and there was also reversal of WSS force vectors. The observance of WSS reversal could generate pathological triggers causing aneurysm initiation

[133]	3 Patient-specific	3 saccular cerebral aneurysms	The impacts of non-Newtonian blood rheology models have been examined.	Using rotational CTA scan	• Two non-Newtonian models (Carreau and Cross) have been used and compared with the Newtonian model	The difference between the two non-Newtonian models and the Newtonian one is higher than the difference between the two non-Newtonian models regarding the velocity magnitude and the WSS
[134]	Ideal	NA	Study the influence of coil embolization on wall loading in terms of pressure and wall shear stress	The geometry considered is a bent tube with a sphere-shaped aneurysm modeled as a bulge located at the central location	• Non-Newtonian fluid using carreau-yasuda model • Womersley velocity profile	The wall shear stress and the wall loading within the aneurysm are greatly diminished. Hence, stabilizes the evolution of the aneurysm
[135]	Ideal	NA	Assess the impacts of coiling embolization on intra-aneurysmal flow and wall shear stress in the dome and neck regions using CFD	NA	• Non-Newtonian fluid using carreau model • flat-profile velocity inlet • Unsteady flow	Coil insertion decreased wall shear stress and its gradient in both the inflow zone and the downstream parent vessel
[136]	1 Patient-specific	1 ICA	The effect of hypertension and modulus of elasticity were analyzed in terms of fluid flow, wall shear stress and pressure	3D-CTA	• Non-Newtonian fluid using Carreau model • Flexible walls • Unsteady flow	High blood pressure and lower modulus of elasticity are important factors that potentiate aneurysm growth and rupture

Table 4
Summary of blood rheology models used with intracranial aneurysm CFD models

Viscosity Model	Constitutive Equation
Newtonian	Constant viscosity ranging from 3.5 mPa to 5mPa [60-60,65-69]
Carreau	$\mu = \mu_\infty + (\mu_0 - \mu_\infty)[1 + (\lambda\dot{\gamma})^2]^{\frac{n-1}{2}}$ μ_∞=0.00345 Pa.s , μ_0=0.056 Pa.s, λ=3.313 s and n=0.3568 [1,37,130] μ_∞=0.0032 Pa.s , μ_0=0.0456 Pa.s, λ=10.03 s and n=0.344 [129]
Carreau–Yasuda	$\mu = \mu_\infty + (\mu_0 - \mu_\infty)[1 + (\lambda\dot{\gamma})^a]^{\frac{n-1}{a}}$ μ_∞=0.0035Pa.s , μ_0=0.16Pa.s, λ=8.2s, a=0.64 and n=0.2128 [126] Carreau A: μ_∞=0.00345Pa.s , μ_0=0.056Pa.s, λ=1.902s, a=1.25 and n=0.22 [102] Carreau B: μ_∞=0.0022Pa.s , μ_0=0.022Pa.s, λ=0.110s, a=0.644 and n=0.392 [102,128,129] $\mu = \mu_\infty + (\mu_0 - \mu_\infty)[1 + (K\dot{\gamma})^2]^n$ μ_∞=0.00345Pa.s , μ_0= 0.056Pa.s, $K = 10.976S^2$ and n = - 0.3216 [32]
Generalized power-law	$\mu = \lambda\dot{\gamma}^{n-1}$

$$\lambda = \mu_\infty + \Delta\mu \; exp\left[-\left(1 + \left(\frac{|\dot{\gamma}|}{a}\right)\right) exp\left(\frac{-b}{|\dot{\gamma}|}\right)\right]$$

$$n = n_\infty - \Delta n \; exp\left[-\left(1 + \left(\frac{|\dot{\gamma}|}{c}\right)\right) exp\left(\frac{-d}{|\dot{\gamma}|}\right)\right]$$

$\mu_\infty = 0.0035 \; Pa.s, \; \Delta\mu = 0.025 \; Pa.s, \; a = 50$
$b = 3, \; c = 50, \; d = 4, \; n_\infty = 1$ and $\Delta n = 0.45$ [60,101-102]

Power-law	$\mu = K\dot{\gamma}^{n-1}$
	$K = 14.67 * 10^{-3} NS^n/m^2$ and n = 0.7755 [40,99]
	$K = 0.0161 \; NS^n/m^2$ and n = 0.63 [124]
Cross	$\mu = \mu_\infty + (\mu_0 - \mu_\infty)/(1 + (\lambda\dot{\gamma})^n)$
	μ_∞=0.0036 Pa.s , μ_0=0.126 Pa.s, n=0.64 and λ=8.2 s [40,67,133]
Walburn-Schneck	$\mu = C_1 e^{(C_2 + C_3/H^2)}\dot{\gamma}^{(1-C_4 H)}$
	C_1=0.00797Pa.s, C_2=0.0608, C_3=377.7515
	and C_4= 0.00499 [40]
Herschel- Bulkley	$\mu = K\dot{\gamma}^{n-1} + \left(\tau_0/\dot{\gamma}\right)$
	$K = 8.9721 * 10^{-3} \; NS^n/m^2$, n=0.8601
	and $\tau_0 = 0.0175 \; N/m^2$ [104,129]
Casson	$\mu = (1/\dot{\gamma})\left[K_0(c) + K_1(c)\sqrt{\dot{\gamma}}\right]^2$
	$K_0(c) = 0.1937 \; (Pa)^{1/2}$,
	$K_1(c) = 0.055 \; (Pa.s)^{1/2}$ [40]
	$\mu = \dfrac{\mu_\infty^2}{\dot{\gamma}} + \dfrac{2\mu_\infty N_\infty}{\sqrt{\dot{\gamma}}} + N_\infty^2$
	$N_\infty = \sqrt{\eta_0(1 - Hct)^{-2.5}}$
	$\mu_\infty = \sqrt{(0.625 Hct)^3}$
	$Hct = 0.4$
	$\eta_0 = 0.00145 \; Pa.s$ [102]
Quemada	$\mu = \mu_\infty\left[1 - \dfrac{1}{2}\left(K_0 + K_\infty\sqrt{\dot{\gamma}/\dot{\gamma}_c}/\left(1 + \sqrt{\dot{\gamma}/\dot{\gamma}_c}\right)\right)\varphi\right]^{-2}$
	$\mu_\infty = 0.0012 Pa.s$, $K_0 = 4.33$, $K_\infty = 2.07$
	$\dot{\gamma}_c = 1.88 \; s^{-1}$ and $\varphi = 0.45$ [40]

3.2.1 Hemodynamic studies using non-newtonian models in intracranial aneurysms

Several studies give credence to the relation between hemodynamic forces and the vessel wall in the genesis of intracranial aneurysm [113-115]. The most debated parameter has been the WSS. Thus, there are various factors including the non-Newtonian blood rheology effect that should be taken into consideration when studying the arterial blood flow.

Studies revealed that WSS is an important hemodynamic factor in intracranial aneurysm genesis, growth and rupture [83, 113, 116, 117]. The most important parameter that affect the WSS is the blood viscosity. Both, low and high WSS paradoxically involved in aneurysm initiation, development and rupture. Most literature showed that the high WSS can be a possible culprit in the formation of IA, when surpass a certain threshold [28, 39, 81, 88, 118, 119], while the low WSS is associated to growth and rupture of IA [28, 39, 81, 88, 118-120]. Moreover, the low WSS may prompt inflammation in the wall and then, the apoptosis of EC, which promote the degradation of the aneurysmal wall and lead to rupture [81, 121, 122].

Most of previous works proved that there is an overestimation of the WSS, when neglecting the effect of the shear-thinning in the simulation [44, 47]. Leuan *et al.,* [43] found that the use of Newtonian fluid can give WSS values three times greater than those produced by the non-Newtonian fluids. On the contrary, some discovered that there is an underestimation of the WSS by neglecting

the shear-thinning [123, 124]. Figures 5-7 show the average WSS, maximum WSS and minimum WSS respectively of the Newtonian model compared to the non-Newtonian model [40, 41, 99, 102, 125].
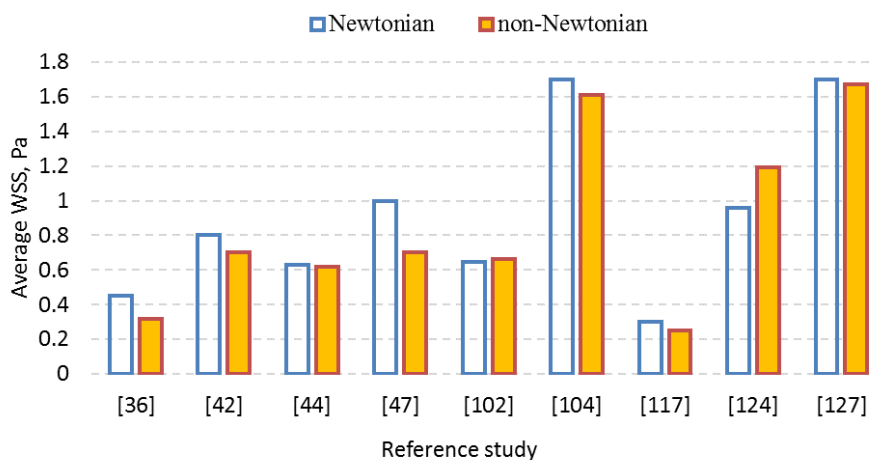

Fig. 5. Comparison of average WSS reported in Newtonian and non-Newtonian models

Previous studies have reported that the non-Newtonian assumption are more accurate and significant to model the blood hemodynamics [62]. Surprisingly, most Newtonian models produce higher average WSS values than the non-Newtonian models, as shown in figure 5. In addition, all the non-Newtonian models have lower maximum and minimum WSS values than the Newtonian as shown in figures 6 and 7 respectively. Thereby, the non-Newtonian effect cannot be neglected so as to avoid overestimating WSS. The effect of the blood rheology on the WSS has been assessed in a patient-specific middle intracranial aneurysm by comparing the Carreau-Yasuda model to the Newtonian model [126]. It is concluded that the oscillatory WSS that indicate the damage of the aneurysm is 0.94 Pa in the Carreau-Yasuda case and 1.56 Pa in the Newtonian case and in the non-oscillatory case, the results obtaining were the same.
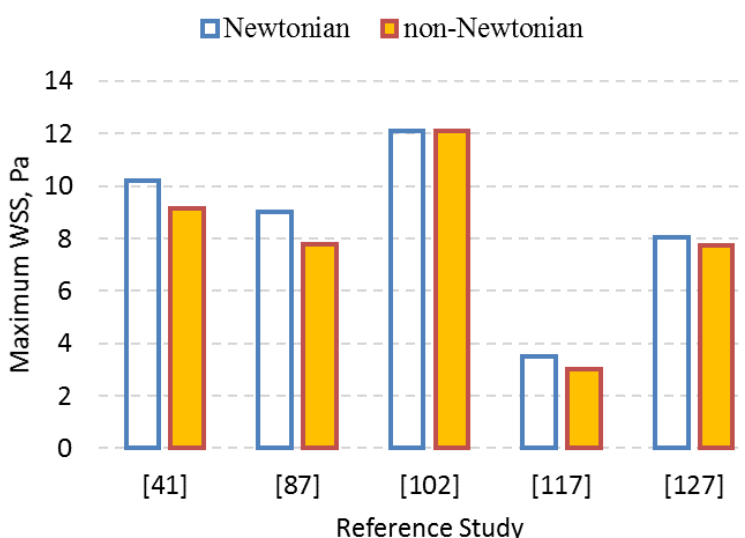

Fig. 6. Comparison of maximum WSS reported in Newtonian and non-Newtonian models
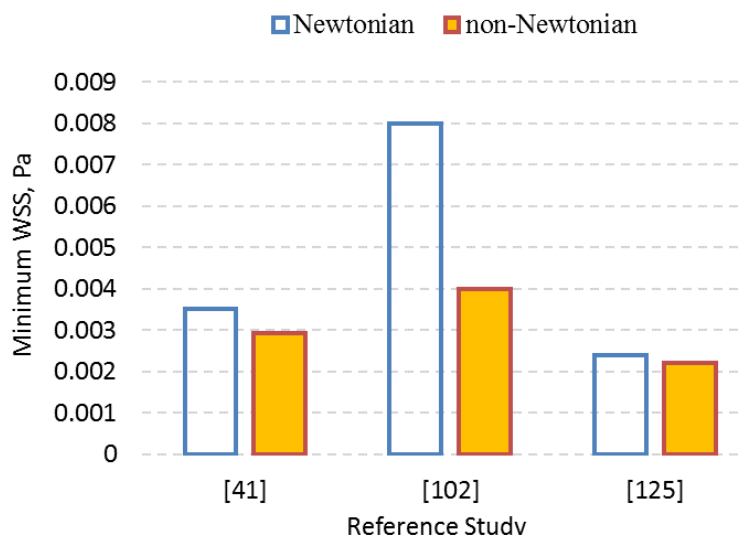
Fig.7. Comparison of minimum WSS reported in Newtonian and non-Newtonian models

Suzuki *et al.,* [46] studied the differences between the commonly used Newtonian model and the non-Newtonian model on the WSS in three different sized intracranial aneurysm models. They normalized the time-averaged WSS distributions by the WSS values obtained with the Newtonian model. All the results obtained with the Newtonian model show a distribution of 1 because WSS in these cases was divided by itself. The results obtained with the non-Newtonian model show areas of markedly increased WSS. However, there are also areas where WSS is lower than that obtained with the Newtonian model. Therefore, the distributions show a mix of regions where the Newtonian model overestimates WSS and regions where the model underestimates WSS. Furthermore, the effect of four non-Newtonian models (Casson, generalized power law, and the two form of Carreau models) have been investigated by studying the WSS of cerebral aneurysms [102]. It is found that all the non-Newtonian models report a lower WSS than that obtained with a Newtonian model in the same geometry. Additionally, they found that the Carreau model is the most conservative predictor of aneurysm vulnerability as well. From this study, the non-Newtonian effects are found to be more significant in aneurysms at bifurcations than in sidewall aneurysms, and also more influential within aneurysms than in the parent vessel. On the contrary, Xiang *et al.,* [47] found that the Newtonian fluid assumption is satisfactory in CFD simulation of healthy vessels and aneurysms that do not harbor regions of pronounced low shear. Although, the non-Newtonian characteristics of blood should be taken into account when modeling the flow dynamics in aneurysms with low shear flow, which are located in aneurysms with complex geometries.

Carty *et al.,* [127] computed the WSS of a CA by studying the effects of non-Newtonian viscosity model and compared with a Newtonian model. The study revealed that the value of WSS of a CA was significantly affected by the non-Newtonian blood analog within low-shear-rate areas which is 42% lesser than the Newtonian one. In addition, they found that the endothelial cells that are exposed to high levels of WSS are more prone to vasculature diseases. Thus, the impact of non-Newtonian viscosity model is very crucial and effective especially for blood flow in low-shear-rate areas in a CA. Bernsdorf and Wang [128] applied the Carreau-Yasuda model to catch the shear-thinning rheology of blood and they calculated the WSS for both Newtonian and non-Newtonian flows at different Reynolds number by using the lattice Boltzmann method. They found that the non-Newtonian behavior of blood can cause the decrement of viscosity in proximity to the wall and also the decrement of WSS comparing to the Newtonian model at a range of Reynolds number. However,

Bernsdorf and Wang [129] found an overestimation of WSS by approximately 30% when ignoring the shear-thinning effects.

Valencia *et al.,* [130] observed that the impact of the shear-thinning rheology are significant only in zones with high velocity gradients which show great spatial and temporal alterations on aneurysmal wall. However, on the aneurysmal wall, results are the same between Newtonian and non-Newtonian blood flow.

The non-Newtonian effect was studied using the Carreau viscosity model by [131] in 3 sidewall aneurysms. It was found that the WSS is low before the formation of the aneurysm and then, the WSS oscillated between maximum and minimum values coinciding with systolic and diastolic cardiac phases. Additionally, there was a reversal of WSS vectors which create the initial stage causing aneurysm genesis. On the other hand, Goodarzi *et al.,* [132] found that there were small alterations on the WSS and WSS divergence when studying the near-wall velocity field of three aneurysms by using the generalized Carreau model versus the Newtonian model. They concluded that the non-Newtonian effects on the flow pattern could be neglected.

Moreover, the effect of two shear-thinning models (Carreau and Cross) for blood has been determined and compared with the standard Newtonian model by using three different realistic geometries of saccular aneurysm obtained from CTA [133]. It is noted that the difference between the two non-Newtonian models and the Newtonian one is higher than the difference between the two non-Newtonian models regarding the velocity magnitude and the WSS. However, the Newtonian model has the greatest pressure drop, which indicates greater viscous forces than those of the non-Newtonian ones. So, the selection of the viscosity model can play a noticeable role in the results.

Hippelheuser *et al.,* [42] examined the hemodynamic forces within 26 patient-specific cerebral aneurysms in the case of bleb formation by studying the impact of the Newtonian and the non-Newtonian (Carreau) viscosity models. The analysis demonstrated that using the Newtonian simplification of constant viscosity yielded no statistical differences between aneurysms with and without blebs, and resulted in greater TAWSS. On the other hand, for the non-Newtonian analysis, aneurysms with blebs showed significantly lower 5% TAWSS compared to those without.

3.2.2 Applications to IA therapy

The influence of coil embolization on wall loading in terms of pressure and WSS has been studied numerically in ideal geometry keeping into consideration the non-Newtonian behavior of blood by using the Carreau-Yasuda model [134]. The study revealed that the WSS within the aneurysm is greatly diminished for Reynolds numbers (Re=500 and Re=1500) after coil enrollment, and that the velocity magnitude becomes marginal. In addition, the pressure keeps the same levels before and after the coil. When the wall loading is decreased, the evolution of the aneurysm could be stopped, and thus considered as an advantage. Furthermore, Schirmer *et al.,* [135] assessed the impact of coil insertion on the intra-aneurysmal flow and WSS in the dome and neck regions by using the Carreau model. Results show a crucial role for the coil embolization position on both intra-aneurysmal and parent vessel hemodynamics, with little influence on pressure distribution, and that the effectiveness rank of coil-parallel orientation is greater than the transverse, and also that the transverse is greater than an orthogonal. In addition, coil enrollment decreased WSS as well as its gradients in both the inflow zone and the downstream parent vessel. Moreover, the influence of blood viscosity on the flow within a coiled aneurysm has been investigated [44]. Both Newtonian and non-Newtonian (Casson) models were considered. To conclude, the assumption of a Newtonian model can be suitable only for the high-viscous regions. In addition, the influence of the non-Newtonian viscosity and flow pulsatility has been investigated to differentiate between the most suitable stent designs.

The flow assumed to be non-Newtonian by using the Power Law model. It is found that the non-Newtonian and pulsatile impacts are substantial to include in order to avert the belittling of WSS, to configure the hemodynamics and to more effectively distinguish more between stent designs. A patient-specific intracranial aneurysm has been analyzed to study the effect of hypertension and modulus of elasticity, taking the Non-Newtonian rheology of blood into account. The aneurysm region encountered great stress and deformation, and hence, elevated blood pressure. It is noted that the maximum deformation of the aneurysmal wall increased with the decrement of the wall modulus of elasticity. Therefore, elevated blood pressure and lower modulus of elasticity could be crucial factors which accelerate the aneurysm's growth and rupture [136]. (Readers should refer to Table 3)

4. Conclusion

This review shows clearly the differences between Newtonian and non-Newtonian modeling approaches in the CFD models of intracranial aneurysms. There are numerous discrepancies that can be identified in literature. The staggering discrepancy is found to be the lack of consensus regarding the non-Newtonian model that could best represent blood flow in intracranial aneurysm. On the other hand, the Newtonian assumption, which is widely used in literature, produces overestimations of aneurysm WSS. Therefore, there is no consensus on the patterns of WSS that could lead to rupture or aneurysm growth. The literature reviewed in this paper shows another important discrepancy in the state-of-the-art knowledge of IA hemodynamics. Different studies use different IA models regardless of their anatomical relevance. In other words, in one study, IA models from posterior and anterior locations are compared, in another study cerebral, carotid and vertebral IA models are compared. The physiological and anatomical parameters are neglected in some published studies, which leads to scattered opinions regarding the role of hemodynamics in IA development at large. Thus, blood viscosity models are debated in different studies, with some works claim that the Newtonian assumption is sufficient, however, on no solid ground. Future studies aim to bring CFD models of IA closer to clinical applications should first classify IA models in question according to their physiological, anatomical and morphological relevance. Future studies should also investigate the nature of blood flow in IA and whether or not it exhibits effective non-Newtonian behavior. Fine tuning of non-Newtonian models is also mandatory if the CFD models are intended to present measures of IA growth and rupture.

References

[1] Cornejo, Sergio, Amador Guzmán, Alvaro Valencia, Jose Rodríguez, and Ender Finol. "Flow-induced wall mechanics of patient-specific aneurysmal cerebral arteries: Nonlinear isotropic versus anisotropic wall stress." *Proceedings of the Institution of Mechanical Engineers, Part H: Journal of Engineering in Medicine* 228, no. 1 (2014): 37-48.
[2] Gard, Andrew P. "Every 18 Minutes, A Brain Aneurysm Ruptures." May 3, (2017).
[3] Hop, Jeannette W., Gabriël JE Rinkel, Ale Algra, and Jan van Gijn. "Case-fatality rates and functional outcome after subarachnoid hemorrhage: a systematic review." *Stroke* 28, no. 3 (1997): 660-664.
[4] Keedy, Alexander. "An overview of intracranial aneurysms." *McGill Journal of Medicine: MJM* 9, no. 2 (2006): 141.
[5] Schievink, Wouter I. "Intracranial aneurysms." *New England Journal of Medicine* 336, no. 1 (1997): 28-40.
[6] Rhoton, Jr AL. "The cerebrum. Anatomy." *Neurosurgery* 61, no. 1 Suppl (2007): 37-118.
[7] Basri, Adi Azriff, Shah Mohammed Abdul Khader, Cherian Johny, Raghuvir Pai, Muhammad Zuber, Kamarul Arifin Ahmad, and Zanuldin Ahmad. "Numerical Study of Haemodynamics Behaviour in Normal and Single Stenosed Renal Artery using Fluid–Structure Interaction." *Journal of Advanced Research in Fluid Mechanics and Thermal Sciences* 51, no. 1 (2018): 91-98.
[8] Sforza, Daniel M., Christopher M. Putman, and Juan Raul Cebral. "Hemodynamics of cerebral aneurysms." *Annual review of fluid mechanics* 41 (2009): 91-107.

[9]   Frösen, Juhana, Riikka Tulamo, Anders Paetau, Elisa Laaksamo, Miikka Korja, Aki Laakso, Mika Niemelä, and Juha Hernesniemi. "Saccular intracranial aneurysm: pathology and mechanisms." *Acta neuropathologica* 123, no. 6 (2012): 773-786.

[10]   Humphrey, J. D., and P. B. Canham. "Structure, mechanical properties, and mechanics of intracranial saccular aneurysms." *Journal of elasticity and the physical science of solids* 61, no. 1-3 (2000): 49-81.

[11]   Jamali, Muhammad Sabaruddin Ahmad, and Zuhaila Ismail. "Simulation of Heat Transfer on Blood Flow through a Stenosed Bifurcated Artery." *Journal of Advanced Research in Fluid Mechanics and Thermal Sciences* 60, no. 2 (2019): 310-323.

[12]   Wang, Xiaohong, and Xiaoyang Li. "Biomechanical behaviors of curved artery with flexible wall: A numerical study using fluid–structure interaction method." *Computers in biology and medicine* 41, no. 11 (2011): 1014-1021.

[13]   Foutrakis, George N., Howard Yonas, and Robert J. Sclabassi. "Saccular aneurysm formation in curved and bifurcating arteries." *American Journal of Neuroradiology* 20, no. 7 (1999): 1309-1317.

[14]   Valencia, Alvaro, and Francisco Solis. "Blood flow dynamics and arterial wall interaction in a saccular aneurysm model of the basilar artery." *Computers & structures* 84, no. 21 (2006): 1326-1337.

[15]   Kim, C. H., J. Cervos-Navarro, H. Kikuchi, N. Hashimoto, and F. Hazama. "Degenerative changes in the internal elastic lamina relating to the development of saccular cerebral aneurysms in rats." *Acta neurochirurgica* 121, no. 1-2 (1993): 76-81.

[16]   Sadamasa, Nobutake, Kazuhiko Nozaki, and Nobuo Hashimoto. "Disruption of gene for inducible nitric oxide synthase reduces progression of cerebral aneurysms." *Stroke* 34, no. 12 (2003): 2980-2984.

[17]   Scanarini, M., S. Mingrino, R. Giordano, and A. Baroni. "Histological and ultrastructural study of intracranial saccular aneurysmal wall." *Acta neurochirurgica* 43, no. 3-4 (1978): 171-182.

[18]   Takao, Yamamoto, Otsuka, Suzuki, and Masuda. "Analysis of Cerebral Aneurysms using Computational Fluid Dynamics (CFD)(New Concept in Treatment for Cerebral Aneurysm)*". Japanese Journal of Neurosurgery* 21, no. 4 (2012): 298-305.

[19]   Penn, David L., Ricardo J. Komotar, and E. Sander Connolly. "Hemodynamic mechanisms underlying cerebral aneurysm pathogenesis." *Journal of Clinical Neuroscience* 18, no. 11 (2011): 1435-1438.

[20]   Lee, Robert MKW. "Morphology of cerebral arteries." *Pharmacology & therapeutics* 66, no. 1 (1995): 149-173.

[21]   Drăghia, F., ALINA CĂTĂLINA Drăghia, and D. O. I. N. A. Onicescu. "Electron microscopic study of the arterial wall in the cerebral aneurysms." *Rom J Morphol Embryol* 49 (2008): 101-103.

[22]   Tamura, Tetsuya, Mohammad A. Jamous, Keiko T. Kitazato, Kenji Yagi, Yoshiteru Tada, Masaaki Uno, and Shinji Nagahiro. "Endothelial damage due to impaired nitric oxide bioavailability triggers cerebral aneurysm formation in female rats." *Journal of hypertension* 27, no. 6 (2009): 1284-1292.

[23]   Irie, Keiko, Hitomi Anzai, Masahiko Kojima, Naomi Honjo, Makoto Ohta, Yuichi Hirose, and Makoto Negoro. "Computational fluid dynamic analysis following recurrence of cerebral aneurysm after coil embolization." *Asian journal of neurosurgery* 7, no. 3 (2012): 109.

[24]   Chiu, Jeng-Jiann, and Shu Chien. "Effects of disturbed flow on vascular endothelium: pathophysiological basis and clinical perspectives." *Physiological reviews* 91, no. 1 (2011): 327-387.

[25]   Sforza, D. M., C. M. Putman, S. Tateshima, F. Vinuela, and J. R. Cebral. "Effects of perianeurysmal environment during the growth of cerebral aneurysms: a case study." *American Journal of Neuroradiology* 33, no. 6 (2012): 1115-1120.

[26]   Tanoue, T., S. Tateshima, J. P. Villablanca, F. Viñuela, and K. Tanishita. "Wall shear stress distribution inside growing cerebral aneurysm." *American journal of neuroradiology* 32, no. 9 (2011): 1732-1737.

[27]   Jou, Liang-Der, Gregory Wong, Brad Dispensa, Michael T. Lawton, Randall T. Higashida, William L. Young, and David Saloner. "Correlation between lumenal geometry changes and hemodynamics in fusiform intracranial aneurysms." *American journal of neuroradiology* 26, no. 9 (2005): 2357-2363.

[28]   Boussel, Loic, Vitaliy Rayz, Charles McCulloch, Alastair Martin, Gabriel Acevedo-Bolton, Michael Lawton, Randall Higashida, Wade S. Smith, William L. Young, and David Saloner. "Aneurysm growth occurs at region of low wall shear stress: patient-specific correlation of hemodynamics and growth in a longitudinal study." *Stroke* 39, no. 11 (2008): 2997-3002.

[29]   Sakaki, T., E. Kohmura, T. Kishiguchi, T. Yuguchi, T. Yamashita, and T. Hayakawa. "Loss and apoptosis of smooth muscle cells in intracranial aneurysms studies with in situ DNA end labeling and antibody against single-stranded DNA." *Acta neurochirurgica* 139, no. 5 (1997): 469-475.

[30]   Steinman, David A., Jaques S. Milner, Chris J. Norley, Stephen P. Lownie, and David W. Holdsworth. "Image-based computational simulation of flow dynamics in a giant intracranial aneurysm." *American Journal of Neuroradiology* 24, no. 4 (2003): 559-566.

[31] Algabri, Yousif A., Surapong Chatpun, and Ishkrizat Taib. "An Investigation of Pulsatile Blood Flow in An Angulated Neck of Abdominal Aortic Aneurysm Using Computational Fluid Dynamics." *Journal of Advanced Research in Fluid Mechanics and Thermal Sciences* 57, no. 2 (2019): 265-274.

[32] Wang, Sheng-zhang, Jia-liang Chen, Guang-hong Ding, Gang Lu, and Xiao-long Zhang. "Non-newtonian computational hemodynamics in two patient-specific cerebral aneurysms with daughter saccules." *Journal of Hydrodynamics* 22, no. 5 (2010): 639-646.

[33] Ku, David N., Don P. Giddens, Christopher K. Zarins, and Seymour Glagov. "Pulsatile flow and atherosclerosis in the human carotid bifurcation. Positive correlation between plaque location and low oscillating shear stress." *Arteriosclerosis: An Official Journal of the American Heart Association, Inc.* 5, no. 3 (1985): 293-302.

[34] Evju, Øyvind, and Kent-Andre Mardal. "On the assumption of laminar flow in physiological flows: Cerebral aneurysms as an illustrative example." In *Modeling the Heart and the Circulatory System*, pp. 177-195. Springer, Cham, 2015.

[35] Khan, M. O., K. Valen-Sendstad, and D. A. Steinman. "Narrowing the expertise gap for predicting intracranial aneurysm hemodynamics: impact of solver numerics versus mesh and time-step resolution." *American Journal of Neuroradiology* 36, no. 7 (2015): 1310-1316.

[36] Khan, M. O., D. A. Steinman, and K. Valen-Sendstad. "Non-Newtonian versus numerical rheology: Practical impact of shear-thinning on the prediction of stable and unstable flows in intracranial aneurysms." *International journal for numerical methods in biomedical engineering* 33, no. 7 (2017): e2836.

[37] Cebral, Juan R., Marcelo A. Castro, James E. Burgess, Richard S. Pergolizzi, Michael J. Sheridan, and Christopher M. Putman. "Characterization of cerebral aneurysms for assessing risk of rupture by using patient-specific computational hemodynamics models." *American Journal of Neuroradiology* 26, no. 10 (2005): 2550-2559.

[38] Hoi, Yiemeng, Hui Meng, Scott H. Woodward, Bernard R. Bendok, Ricardo A. Hanel, Lee R. Guterman, and L. Nelson Hopkins. "Effects of arterial geometry on aneurysm growth: three-dimensional computational fluid dynamics study." *Journal of neurosurgery* 101, no. 4 (2004): 676-681.

[39] Meng, Hui, Zhijie Wang, Yiemeng Hoi, Ling Gao, Eleni Metaxa, Daniel D. Swartz, and John Kolega. "Complex hemodynamics at the apex of an arterial bifurcation induces vascular remodeling resembling cerebral aneurysm initiation." *Stroke* 38, no. 6 (2007): 1924-1931.

[40] Campo-Deaño, Laura, Mónica SN Oliveira, and Fernando T. Pinho. "A review of computational hemodynamics in middle cerebral aneurysms and rheological models for blood flow." *Applied Mechanics Reviews* 67, no. 3 (2015): 030801.

[41] Frolov, S. V., S. V. Sindeev, D. Liepsch, and A. Balasso. "Experimental and CFD flow studies in an intracranial aneurysm model with Newtonian and non-Newtonian fluids." *Technology and Health Care* 24, no. 3 (2016): 317-333.

[42] Hippelheuser, James E., Alexandra Lauric, Alex D. Cohen, and Adel M. Malek. "Realistic non-Newtonian viscosity modelling highlights hemodynamic differences between intracranial aneurysms with and without surface blebs." *Journal of biomechanics* 47, no. 15 (2014): 3695-3703.

[43] Ieuan Owen, J. G., Marcel Escudier, and Rob Poole. "The importance of the non-Newtonian characteristics of blood in flow modelling studies." *Journal of Applied Fluid Mechanics* 2 (2009).

[44] Morales, Hernán G., Ignacio Larrabide, Arjan J. Geers, Martha L. Aguilar, and Alejandro F. Frangi. "Newtonian and non-Newtonian blood flow in coiled cerebral aneurysms." *Journal of biomechanics* 46, no. 13 (2013): 2158-2164.

[45] Otani, Tomohiro, Satoshi Ii, Masayuki Hirata, and Shigeo Wada. "Computational study of the non-Newtonian effect of blood on flow stagnation in a coiled cerebral aneurysm." *Nihon Reoroji Gakkaishi* 45, no. 5 (2017): 243-249.

[46] Suzuki, Takashi, Hiroyuki Takao, Takamasa Suzuki, Tomoaki Suzuki, Shunsuke Masuda, Chihebeddine Dahmani, Mitsuyoshi Watanabe et al. "Variability of hemodynamic parameters using the common viscosity assumption in a computational fluid dynamics analysis of intracranial aneurysms." *Technology and Health Care* 25, no. 1 (2017): 37-47.

[47] Xiang, Jianping, Markus Tremmel, John Kolega, Elad I. Levy, Sabareesh K. Natarajan, and Hui Meng. "Newtonian viscosity model could overestimate wall shear stress in intracranial aneurysm domes and underestimate rupture risk." *Journal of neurointerventional surgery* 4, no. 5 (2012): 351-357.

[48] Berg, P., S. Saalfeld, S. Voß, T. Redel, B. Preim, G. Janiga, and O. Beuing. "Does the DSA reconstruction kernel affect hemodynamic predictions in intracranial aneurysms? An analysis of geometry and blood flow variations." *Journal of neurointerventional surgery* 10, no. 3 (2018): 290-296.

[49] Geers, Arjan J., Ignacio Larrabide, A. G. Radaelli, Hrvoje Bogunovic, HAF Gratama Van Andel, C. B. Majoie, and Alejandro F. Frangi. "Reproducibility of image-based computational hemodynamics in intracranial aneurysms: comparison of CTA and 3DRA." In *2009 IEEE International Symposium on Biomedical Imaging: From Nano to Macro*, pp. 610-613. IEEE, 2009.

[50] Schneiders, J. J., H. A. Marquering, L. Antiga, R. Van den Berg, E. VanBavel, and C. B. Majoie. "Intracranial aneurysm neck size overestimation with 3D rotational angiography: the impact on intra-aneurysmal hemodynamics simulated with computational fluid dynamics." *American Journal of Neuroradiology* 34, no. 1 (2013): 121-128.

[51] Robertson, Anne M., Adélia Sequeira, and Marina V. Kameneva. "Hemorheology." In *Hemodynamical flows*, pp. 63-120. Birkhäuser Basel, 2008.

[52] Eckmann, David M., Shelly Bowers, Mark Stecker, and Albert T. Cheung. "Hematocrit, volume expander, temperature, and shear rate effects on blood viscosity." *Anesthesia & Analgesia* 91, no. 3 (2000): 539-545.

[53] Merrill, E. W., E. R. Gilliland, G. Cokelet, H. Shin, A. Britten, and R. E. Wells Jr. "Rheology of blood and flow in the microcirculation." *Journal of applied physiology* 18, no. 2 (1963): 255-260.

[54] Cebral, Juan R., Fernando Mut, Jane Weir, and Christopher Putman. "Quantitative characterization of the hemodynamic environment in ruptured and unruptured brain aneurysms." *American Journal of Neuroradiology* 32, no. 1 (2011): 145-151.

[55] Jou, L-D., Deok Hee Lee, Hesham Morsi, and Michel E. Mawad. "Wall shear stress on ruptured and unruptured intracranial aneurysms at the internal carotid artery." *American Journal of Neuroradiology* 29, no. 9 (2008): 1761-1767.

[56] Cebral, J. R., F. Mut, M. Raschi, E. Scrivano, R. Ceratto, P. Lylyk, and C. M. Putman. "Aneurysm rupture following treatment with flow-diverting stents: computational hemodynamics analysis of treatment." *American journal of neuroradiology* 32, no. 1 (2011): 27-33.

[57] Xiang, Jianping, Sabareesh K. Natarajan, Markus Tremmel, Ding Ma, J. Mocco, L. Nelson Hopkins, Adnan H. Siddiqui, Elad I. Levy, and Hui Meng. "Hemodynamic–morphologic discriminants for intracranial aneurysm rupture." *Stroke* 42, no. 1 (2011): 144-152.

[58] Stuart, John, and Martin W. Kenny. "Blood rheology." *Journal of clinical pathology* 33, no. 5 (1980): 417.

[59] Mejia, Juan, Rosaire Mongrain, and Olivier F. Bertrand. "Accurate prediction of wall shear stress in a stented artery: Newtonian versus non-Newtonian models." *Journal of biomechanical engineering* 133, no. 7 (2011): 074501.

[60] Johnston, Barbara M., Peter R. Johnston, Stuart Corney, and David Kilpatrick. "Non-Newtonian blood flow in human right coronary arteries: transient simulations." *Journal of biomechanics* 39, no. 6 (2006): 1116-1128.

[61] Mallik, B. Basu, Saktipada Nanda, Bhabatosh Das, Debanshu Saha, Debanu Shankar Das, and Koustav Paul. "A non-Newtonian fluid model for blood flow using power-law through an atherosclerotic arterial segment having slip velocity." *International journal of pharmaceutical, chemical and biological sciences* 3, no. 3 (2013): 752-760.

[62] Mandal, Prashanta Kumar. "An unsteady analysis of non-Newtonian blood flow through tapered arteries with a stenosis." *International Journal of Non-Linear Mechanics* 40, no. 1 (2005): 151-164.

[63] Jeong, W. W., and K. Rhee. "Effects of surface geometry and non-newtonian viscosity on the flow field in arterial stenoses." *Journal of mechanical science and technology* 23, no. 9 (2009): 2424-2433.

[64] K Kulcsár, Zsolt Mihály. "Role of hemodynamics in the life cycle of cerebral aneurysm." *Semmelweis University, PhD Thesis* (2011).

[65] Lindekleiv, Haakon M., Kristian Valen-Sendstad, Michael K. Morgan, Kent-Andre Mardal, Kenneth Faulder, Jeanette H. Magnus, Knut Waterloo, Bertil Romner, and Tor Ingebrigtsen. "Sex differences in intracranial arterial bifurcations." *Gender medicine* 7, no. 2 (2010): 149-155.

[66] Anand, M., and K. R. Rajagopal. "A shear-thinning viscoelastic fluid model for describing the flow of blood." *Int. J. Cardiovasc. Med. Sci* 4, no. 2 (2004): 59-68.

[67] Bodnár, T., A. Sequeira, and L. Pirkl. "Numerical Simulations of Blood Flow in a Stenosed Vessel under Different Flow Rates using a Generalized Oldroyd-B Model." In *AIP Conference Proceedings*, vol. 1168, no. 1, pp. 645-648. AIP, 2009.

[68] Kouhi, E., Y. S. Morsi, and S. H. Masood. "Haemodynamic analysis of coronary artery bypass grafting in a non-linear deformable artery and Newtonian pulsatile blood flow." *Proceedings of the Institution of Mechanical Engineers, Part H: Journal of Engineering in Medicine* 222, no. 8 (2008): 1273-1287.

[69] Lee, K. W., and X. Y. Xu. "Modelling of flow and wall behaviour in a mildly stenosed tube." *Medical engineering & physics* 24, no. 9 (2002): 575-586.

[70] Saqr, Khalid M., Ossama Mansour, Simon Tupin, Tamer Hassan, and Makoto Ohta. "Evidence for non-Newtonian behavior of intracranial blood flow from Doppler ultrasonography measurements." *Medical & biological engineering & computing* 57, no. 5 (2019): 1029-1036.

[71] Stojanović, Nebojša, Ivan Stefanović, Saša Ranđelović, Rade Mitić, Petar Bošnjaković, and Dragan Stojanov. "Presence of anatomical variations of the circle of Willis in patients undergoing surgical treatment for ruptured intracranial aneurysms." *Vojnosanitetski pregled* 66, no. 9 (2009): 711-717.

[72] Kayembe, K. N., Masakiyo Sasahara, and Fumitada Hazama. "Cerebral aneurysms and variations in the circle of Willis." *Stroke* 15, no. 5 (1984): 846-850.

[73] Zarins, Christopher K., Don P. Giddens, B. K. Bharadvaj, Vikrom S. Sottiurai, Robert F. Mabon, and Seymour Glagov. "Carotid bifurcation atherosclerosis. Quantitative correlation of plaque localization with flow velocity profiles and wall shear stress." *Circulation research* 53, no. 4 (1983): 502-514.

[74] Castro, M. A., Christopher M. Putman, and J. R. Cebral. "Computational fluid dynamics modeling of intracranial aneurysms: effects of parent artery segmentation on intra-aneurysmal hemodynamics." *American Journal of Neuroradiology* 27, no. 8 (2006): 1703-1709.

[75] Wang, Qing, Wei-zhe Wang, Zhi-min Fei, Ying-zheng Liu, and Zhao-min Cao. "Simulation of blood flow in intracranial ICA-pcoma aneurysm via computational fluid dymamics modeling." *Journal of Hydrodynamics* 21, no. 5 (2009): 583-590.

[76] Alnæs, Martin Sandve, Jørgen Isaksen, Kent-André Mardal, Bertil Romner, Michael K. Morgan, and Tor Ingebrigtsen. "Computation of hemodynamics in the circle of Willis." *Stroke* 38, no. 9 (2007): 2500-2505.

[77] Isaksen, Jørgen Gjernes, Yuri Bazilevs, Trond Kvamsdal, Yongjie Zhang, Jon H. Kaspersen, Knut Waterloo, Bertil Romner, and Tor Ingebrigtsen. "Determination of wall tension in cerebral artery aneurysms by numerical simulation." *Stroke* 39, no. 12 (2008): 3172-3178.

[78] Valen-Sendstad, Kristian, Kent-André Mardal, Mikael Mortensen, Bjørn Anders Pettersson Reif, and Hans Petter Langtangen. "Direct numerical simulation of transitional flow in a patient-specific intracranial aneurysm." *Journal of biomechanics* 44, no. 16 (2011): 2826-2832.

[79] Sforza, D. M., C. M. Putman, E. Scrivano, P. Lylyk, and J. R. Cebral. "Blood-flow characteristics in a terminal basilar tip aneurysm prior to its fatal rupture." *American Journal of Neuroradiology* 31, no. 6 (2010): 1127-1131.

[80] Chien, A., M. A. Castro, S. Tateshima, J. Sayre, J. Cebral, and F. Vinuela. "Quantitative hemodynamic analysis of brain aneurysms at different locations." *American Journal of Neuroradiology* 30, no. 8 (2009): 1507-1512.

[81] Shojima, Masaaki, Marie Oshima, Kiyoshi Takagi, Ryo Torii, Motoharu Hayakawa, Kazuhiro Katada, Akio Morita, and Takaaki Kirino. "Magnitude and role of wall shear stress on cerebral aneurysm: computational fluid dynamic study of 20 middle cerebral artery aneurysms." *Stroke* 35, no. 11 (2004): 2500-2505.

[82] Raschi, Marcelo, Fernando Mut, Greg Byrne, Christopher M. Putman, Satoshi Tateshima, Fernando Viñuela, Tetsuya Tanoue, Kazuo Tanishita, and Juan R. Cebral. "CFD and PIV analysis of hemodynamics in a growing intracranial aneurysm." *International journal for numerical methods in biomedical engineering* 28, no. 2 (2012): 214-228.

[83] Singh, Pankaj K., Alberto Marzo, Bethany Howard, Daniel A. Rufenacht, Philippe Bijlenga, Alejandro F. Frangi, Patricia V. Lawford, Stuart C. Coley, D. Rodney Hose, and Umang J. Patel. "Effects of smoking and hypertension on wall shear stress and oscillatory shear index at the site of intracranial aneurysm formation." *Clinical neurology and neurosurgery* 112, no. 4 (2010): 306-313.

[84] Bowker, T. J., P. N. Watton, P. E. Summers, J. V. Byrne, and Y. Ventikos. "Rest versus exercise hemodynamics for middle cerebral artery aneurysms: a computational study." *American Journal of Neuroradiology* 31, no. 2 (2010): 317-323.

[85] Baek, H., M. V. Jayaraman, P. D. Richardson, and G. E. Karniadakis. "Flow instability and wall shear stress variation in intracranial aneurysms." *Journal of the Royal Society Interface* 7, no. 47 (2009): 967-988.

[86] Jou, Liang-Der, Christopher M. Quick, William L. Young, Michael T. Lawton, Randall Higashida, Alastair Martin, and David Saloner. "Computational approach to quantifying hemodynamic forces in giant cerebral aneurysms." *American Journal of Neuroradiology* 24, no. 9 (2003): 1804-1810.

[87] Hassan, Tamer, Eugene V. Timofeev, Tsutomu Saito, Hiroaki Shimizu, Masayuki Ezura, Yasushi Matsumoto, Kazuyoshi Takayama, Teiji Tominaga, and Akira Takahashi. "A proposed parent vessel geometry—based categorization of saccular intracranial aneurysms: computational flow dynamics analysis of the risk factors for lesion rupture." *Journal of neurosurgery* 103, no. 4 (2005): 662-680.

[88] Ujiie, Hiroshi, Hiroyuki Tachi, Osamu Hiramatsu, Andrew L. Hazel, Takeshi Matsumoto, Yasuo Ogasawara, Hiroshi Nakajima, Tomokatsu Hori, Kintomo Takakura, and Fumihiko Kajiya. "Effects of size and shape (aspect ratio) on the hemodynamics of saccular aneurysms: a possible index for surgical treatment of intracranial aneurysms." *Neurosurgery* 45, no. 1 (1999): 119-130.

[89] Cebral, Juan R., Marcelo Adrián Castro, Sunil Appanaboyina, Christopher M. Putman, Daniel Millan, and Alejandro F. Frangi. "Efficient pipeline for image-based patient-specific analysis of cerebral aneurysm hemodynamics: technique and sensitivity." *IEEE transactions on medical imaging* 24, no. 4 (2005): 457-467.

[90] Beck, J., S. Rohde, M. El Beltagy, M. Zimmermann, J. Berkefeld, V. Seifert, and A. Raabe. "Difference in configuration of ruptured and unruptured intracranial aneurysms determined by biplanar digital subtraction angiography." *Acta neurochirurgica* 145, no. 10 (2003): 861-865.

[91] Forget Jr, Thomas R., Ronald Benitez, Erol Veznedaroglu, Ashwini Sharan, William Mitchell, Marco Silva, and Robert H. Rosenwasser. "A review of size and location of ruptured intracranial aneurysms." *Neurosurgery* 49, no. 6 (2001): 1322-1326.

[92] Raghavan, Madhavan L., Baoshun Ma, and Robert E. Harbaugh. "Quantified aneurysm shape and rupture risk." *Journal of neurosurgery* 102, no. 2 (2005): 355-362.

[93] Rinkel, Gabriel JE, Mamuka Djibuti, Ale Algra, and J. Van Gijn. "Prevalence and risk of rupture of intracranial aneurysms: a systematic review." *Stroke* 29, no. 1 (1998): 251-256.

[94] Weir, Bryce, Lew Disney, and Theodore Karrison. "Sizes of ruptured and unruptured aneurysms in relation to their sites and the ages of patients." *Journal of neurosurgery* 96, no. 1 (2002): 64-70.

[95] ORZ, S. KOBAYASHI, M. OSAWA & Y. TANAKA, Y. "Aneurysm size: a prognostic factor for rupture." *British journal of neurosurgery* 11, no. 2 (1997): 144-149.

[96] Carter, Bob S., Sunil Sheth, Eric Chang, Manish Sethl, and Christopher S. Ogilvy. "Epidemiology of the size distribution of intracranial bifurcation aneurysms: smaller size of distal aneurysms and increasing size of unruptured aneurysms with age." *Neurosurgery* 58, no. 2 (2006): 217-223.

[97] Castro, M. A., C. M. Putman, M. J. Sheridan, and J. R. Cebral. "Hemodynamic patterns of anterior communicating artery aneurysms: a possible association with rupture." *American journal of neuroradiology* 30, no. 2 (2009): 297-302.

[98] Cebral, J. R., M. Sheridan, and C. M. Putman. "Hemodynamics and bleb formation in intracranial aneurysms." *American Journal of Neuroradiology* 31, no. 2 (2010): 304-310.

[99] Molla and Paul, "*LES of non-Newtonian physiological blood flow in a model of arterial stenosis".* Medical Engineering & Physics. 34**,** no. 8 (2012): p. 1079-87.

[100] Yilmaz, Fuat, and Mehmet Yasar Gundogdu. "A critical review on blood flow in large arteries; relevance to blood rheology, viscosity models, and physiologic conditions." *Korea-Australia Rheology Journal* 20, no. 4 (2008): 197-211.

[101] Husain, I., C. Langdon, and J. Schwark. "Non-Newtonian pulsatile blood flow in a modeled artery with a stenosis and an aneurysm." *Rec. Res. Envi. Geo. Sc*: 413-418.

[102] Fisher, Carolyn, and Jenn Stroud Rossmann. "Effect of non-Newtonian behavior on hemodynamics of cerebral aneurysms." *Journal of biomechanical engineering* 131, no. 9 (2009): 091004.

[103] Perktold, Karl, R. Peter, and Michael Resch. "Pulsatile non-Newtonian blood flow simulation through a bifurcation with an aneurysm." *Biorheology* 26, no. 6 (1989): 1011-1030.

[104] Valencia, Alvaro A., Amador M. Guzmán, Ender A. Finol, and Cristina H. Amon. "Blood flow dynamics in saccular aneurysm models of the basilar artery." *Journal of biomechanical engineering* 128, no. 4 (2006): 516-526.

[105] Steinman, David A. "Assumptions in modelling of large artery hemodynamics." In *Modeling of physiological flows*, pp. 1-18. Springer, Milano, 2012.

[106] Rayz, V. L., L. Boussel, M. T. Lawton, G. Acevedo-Bolton, L. Ge, W. L. Young, R. T. Higashida, and D. Saloner. "Numerical modeling of the flow in intracranial aneurysms: prediction of regions prone to thrombus formation." *Annals of biomedical engineering* 36, no. 11 (2008): 1793.

[107] Arzani, Amirhossein. "Accounting for residence-time in blood rheology models: do we really need non-Newtonian blood flow modelling in large arteries?." *Journal of The Royal Society Interface* 15, no. 146 (2018): 20180486.

[108] Sochi, Taha. "Non-Newtonian rheology in blood circulation." *arXiv preprint arXiv:1306.2067* (2013).

[109] Sankar, D. S., and Yazariah Yatim. "Comparative analysis of mathematical models for blood flow in tapered constricted arteries." In *Abstract and Applied Analysis*, vol. 2012. Hindawi, 2012.

[110] Madlener, K., B. Frey, and H. K. Ciezki. "Generalized reynolds number for non-newtonian fluids." *Progress in Propulsion Physics* 1 (2009): 237-250.

[111] Passerini, Tiziano, Annalisa Quaini, Umberto Villa, Alessandro Veneziani, and Suncica Canic. "Validation of an open source framework for the simulation of blood flow in rigid and deformable vessels." *International journal for numerical methods in biomedical engineering* 29, no. 11 (2013): 1192-1213.

[112] Mikhal, Julia. "Modeling and simulation of flow in cerebral aneurysms." *University of Twente, Enschede* (2012).

[113] Burleson, Arrmelle C., and Vincent T. Turitto. "Identification of quantifiable hemodynamic factors in the assessment of cerebral aneurysm behavior on behalf of the subcommittee on biorheology of the scientific and standardization committee of the ISTH." *Thrombosis and haemostasis* 75, no. 01 (1996): 118-123.

[114] Gao, Ling, Yiemeng Hoi, Daniel D. Swartz, John Kolega, Adnan Siddiqui, and Hui Meng. "Nascent aneurysm formation at the basilar terminus induced by hemodynamics." *Stroke* 39, no. 7 (2008): 2085-2090.

[115] Morimoto, Masafumi, Susumu Miyamoto, Akira Mizoguchi, Noriaki Kume, Toru Kita, and Nobuo Hashimoto. "Mouse model of cerebral aneurysm: experimental induction by renal hypertension and local hemodynamic changes." *Stroke* 33, no. 7 (2002): 1911-1915.

[116] Shojima, Masaaki, Shigeru Nemoto, Akio Morita, Marie Oshima, Eiju Watanabe, and Nobuhito Saito. "Role of shear stress in the blister formation of cerebral aneurysms." *Neurosurgery* 67, no. 5 (2010): 1268-1275.

[117] Evju, Øyvind, Kristian Valen-Sendstad, and Kent-André Mardal. "A study of wall shear stress in 12 aneurysms with respect to different viscosity models and flow conditions." *Journal of biomechanics* 46, no. 16 (2013): 2802-2808.

[118] Kondo, Soichiro. "Cerebral Aneurysms Arising at Non-branching Sites: An Experimental Study." *Stroke* 28, no. 2 (1997): 398.

[119] Fukuda, Shunichi, Nobuo Hashimoto, Hiroaki Naritomi, Izumi Nagata, Kazuhiko Nozaki, Soichiro Kondo, Michiharu Kurino, and Haruhiko Kikuchi. "Prevention of rat cerebral aneurysm formation by inhibition of nitric oxide synthase." *Circulation* 101, no. 21 (2000): 2532-2538.

[120] Miura, Yoichi, Fujimaro Ishida, Yasuyuki Umeda, Hiroshi Tanemura, Hidenori Suzuki, Satoshi Matsushima, Shinichi Shimosaka, and Waro Taki. "Low wall shear stress is independently associated with the rupture status of middle cerebral artery aneurysms." *Stroke* 44, no. 2 (2013): 519-521.

[121] Meng, H., V. M. Tutino, J. Xiang, and A. Siddiqui. "High WSS or low WSS? Complex interactions of hemodynamics with intracranial aneurysm initiation, growth, and rupture: toward a unifying hypothesis." *American Journal of Neuroradiology* 35, no. 7 (2014): 1254-1262.

[122] Tateshima, S., K. Tanishita, H. Omura, J. P. Villablanca, and F. Vinuela. "Intra-aneurysmal hemodynamics during the growth of an unruptured aneurysm: in vitro study using longitudinal CT angiogram database." *American journal of neuroradiology* 28, no. 4 (2007): 622-627.

[123] Cavazzuti, Marco, Mark Atherton, Michael Collins, and Giovanni Barozzi. "Beyond the virtual intracranial stenting challenge 2007: non-Newtonian and flow pulsatility effects." *Journal of biomechanics* 43, no. 13 (2010): 2645-2647.

[124] Cavazzuti, Marco, M. A. Atherton, M. W. Collins, and Giovanni Sebastiano Barozzi. "Non-Newtonian and flow pulsatility effects in simulation models of a stented intracranial aneurysm." *Proceedings of the Institution of Mechanical Engineers, Part H: Journal of Engineering in Medicine* 225, no. 6 (2011): 597-609.

[125] Huang, Changsheng, Zhenhua Chai, and Baochang Shi. "Non-newtonian effect on hemodynamic characteristics of blood flow in stented cerebral aneurysm." *Communications in Computational Physics* 13, no. 3 (2013): 916-928.

[126] Bernabeu, Miguel O., Rupert W. Nash, Derek Groen, Hywel B. Carver, James Hetherington, Timm Krüger, and Peter V. Coveney. "Impact of blood rheology on wall shear stress in a model of the middle cerebral artery." *Interface Focus* 3, no. 2 (2013): 20120094.

[127] Carty, Gregory, Surapong Chatpun, and Daniel M. Espino. "Modeling blood flow through intracranial aneurysms: A comparison of Newtonian and non-Newtonian viscosity." *Journal of Medical and Biological Engineering* 36, no. 3 (2016): 396-409.

[128] Bernsdorf, Jörg, and Dinan Wang. "Non-Newtonian blood flow simulation in cerebral aneurysms." *Computers & Mathematics with Applications* 58, no. 5 (2009): 1024-1029.

[129] B Bernsdorf, Jürg, and Dinan Wang. "Blood flow simulation in cerebral aneurysm: A lattice Boltzmann application in medical physics." In *Parallel Computational Fluid Dynamics 2007*, pp. 291-296. Springer, Berlin, Heidelberg, 2009.

[130] Valencia, Alvaro, Alvaro Zarate, Marcelo Galvez, and Lautaro Badilla. "Non-Newtonian blood flow dynamics in a right internal carotid artery with a saccular aneurysm." *International Journal for Numerical Methods in Fluids* 50, no. 6 (2006): 751-764.

[131] Mantha, A., Christof Karmonik, G. Benndorf, C. Strother, and Ralph Metcalfe. "Hemodynamics in a cerebral artery before and after the formation of an aneurysm." *American Journal of Neuroradiology* 27, no. 5 (2006): 1113-1118.

[132] Goodarzi Ardakani, Vahid, Xin Tu, Alberto M. Gambaruto, Iolanda Velho, Jorge Tiago, Adélia Sequeira, and Ricardo Pereira. "Near-Wall Flow in Cerebral Aneurysms." *Fluids* 4, no. 2 (2019): 89.

[133] Gambaruto, Alberto, João Janela, Alexandra Moura, and Adélia Sequeira. "Shear-thinning effects of hemodynamics in patient-specific cerebral aneurysms." *Mathematical biosciences and engineering: MBE* 10, no. 3 (2013): 649-665.

[134] Agrawal, Vishal, Chandan Paul, M. K. Das, and K. Muralidhar. "Effect of coil embolization on blood flow through a saccular cerebral aneurysm." *Sadhana* 40, no. 3 (2015): 875-887.

[135] Schirmer, Clemens M., and Adel M. Malek. "Critical influence of framing coil orientation on intra-aneurysmal and neck region hemodynamics in a sidewall aneurysm model." *Neurosurgery* 67, no. 6 (2010): 1692-1702.

[136] Ahmed, S., I. D. Šutalo, H. Kavnoudias, and A. Madan. "Fluid structure interaction modelling of a patient specific cerebral aneurysm: effect of hypertension and modulus of elasticity." (2007): 75-81.